J|A|C|S COMMUNICATIONS

Published on Web 04/29/2010

Postchemistry of Organic Particles: When TTF Microparticles Meet TCNQ Microstructures in Aqueous Solution

Jinchong Xiao,[†] Zongyou Yin,[†] Hong Li,[‡] Qing Zhang,[‡] Freddy Boey,[†] Hua Zhang,[†] and Qichun Zhang*,[†]

School of Materials Science and Engineering, Nanyang Technological University, 50 Nanyang Avenue, Singapore 639798, and Microelectronics Center, School of Electrical and Electronics Engineering, Nanyang Technological University, Singapore 639798

Received March 15, 2010; E-mail: qczhang@ntu.edu.sg

The conversion of preformed inorganic nanoparticles into more complicated nanocrystalline solids has been shown to be a viable process for enriching compositional and morphological complexity in the inorganic nanoworld.[1] As a counterpart, organic particles should also possess this potential to perform chemical conversion since the building blocks in organic micro/nanomaterials have relatively weaker interactions. Nevertheless, the present reports for organic particles focus only on their synthesis (shape and size control) and applications.[2] Although many methods[3−7] for creating different morphologies of organic micro/nanomaterials have been developed, the use of organic particles as starting materials to generate novel organic micro/nanostructures through chemical conversion/transformation is unprecedented. This gap in knowledge strongly encouraged us to explore the possibility of this concept in organic materials.

The materials chosen for this work were aqueous tetrathiafulvalene (TTF) microparticles and 7,7′,8,8′-tetracyanoquinodimethane (TCNQ) microstructures. TTF−TCNQ is a well-known organic charge-transfer (CT) salt that has a well-defined quasi-one-dimensional structure with a high electronic conductivity.[8] Especially, the recent reobservation of metallic conductivity at the interface between two crystals of TTF and TCNQ through direct mechanical contact offers a novel method for preparing new organic electronic systems with possible novel physical phenomena.[9]

Rather than focusing on the bulk TTF−TCNQ and their properties, we were more interested in the postchemistry between aqueous TTF microparticles and TCNQ microstructures. It should be noted that this is the first observation of a chemical reaction occurring in aqueous organic micro/nanoparticles. Previous work has focused only on the chemical activity of organic micro/nanostructures for sensors[10] or simple chemical doping to tune their electronic/optical properties.[11,12]

The aqueous TTF microparticles (or TCNQ microstructures) were prepared by adding a TTF (or TCNQ) acetonitrile solution to water containing poly(ethylene glycol)-*block*-poly(propylene glycol)-*block*-poly(ethylene glycol) (P123) nonionic surfactant. The formation of TTF−TCNQ nanowires could be observed after the addition of aqueous TTF microparticles to a TCNQ aqueous solution. After 1 day, deposition of as-synthesized TTF−TCNQ nanowires was observed.

Figure 1a shows a typical scanning electron microscopy (SEM) image of TTF microparticles with a relatively broad size distribution (500 nm to 1.2 μm), while TCNQ microstructures (shown in Figure 1b) have a relatively narrow size arrangement (500−800 nm). When TTF microparticles were added to TCNQ microstructures in aqueous solution, the color of the TCNQ solution immediately changed from yellow-green to brown (Figure 2a inset), and TTF−TCNQ nanowires were formed. The SEM images (Figure 1c,d) show that the diameters and lengths of the TTF−TCNQ nanowires were 300−700 nm and >10 μm, respectively.

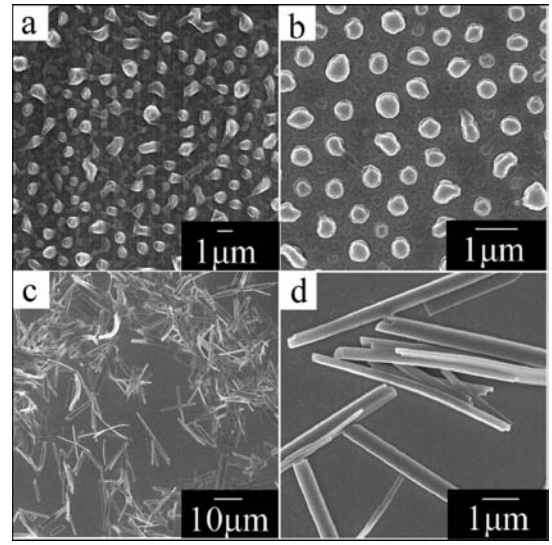

Figure 1. SEM images of (a) TTF microparticles, (b) TCNQ microstructures, and (c, d) TTF−TCNQ nanowires.

Figure 2a shows the UV−vis absorption spectra of TCNQ microstructures (red), TTF microparticles (black), and TTF−TCNQ nanowires (blue) measured in aqueous solution. The TTF microparticles showed two broad absorption peaks at 315 and 375 nm instead of three peaks (290 nm, 310 and 365 nm) as previously reported for TTF molecules in organic solution.[13] Interestingly, the absorption spectrum of TCNQ microparticles in aqueous solution was very similar to that of TCNQ molecules in organic solution, with two peaks at 400 nm (main peak) and 375 nm (shoulder peak).[14] The UV absorption spectrum of TTF−TCNQ nanowires showed the presence of TTF radical cations (330, 430, and 650−700 nm)[13,15,16] and TCNQ radical anions (700−800 and 800−900 nm).[14]

All of the samples were characterized and confirmed by X-ray diffraction (XRD), and the results are shown in Figure S1 in the Supporting Information. The XRD pattern of the TCNQ microstructures was indexed in space group $C2/c$, in agreement with previously reported results with "standard" lattice constants (a = 8.915 Å, b = 7.065 Å, c = 16.399 Å, β = 98.50°),[17] while the TTF microparticles yielded an XRD pattern similar to one with the following published lattice parameters: $P2_1/c$, a = 7.358 Å, b = 4.019 Å, c = 13.911 Å, β = 101.427°.[18] The XRD analysis of

[†] School of Materials Science and Engineering.
[‡] School of Electrical and Electronics Engineering.

10.1021/ja102154b © 2010 American Chemical Society

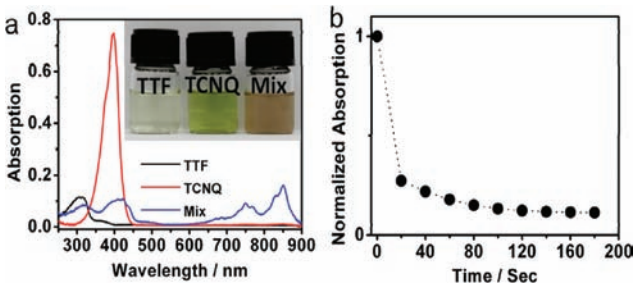

Figure 2. (a) UV−vis absorption spectra of TCNQ microstructures (red), TTF microparticles (black), and TTF−TCNQ nanowires (blue). The inset shows vials containing TCNQ microstructures, TTF microparticles, and TTF−TCNQ nanowires in aqueous solution. (b) Absorption variation of TCNQ microstructures as a function of reaction time after mixing of the TTF microparticles and TCNQ microstructures.

TTF−TCNQ nanowires showed that the complexes had high crystallinity with cell data ($P2_1/c$, $a = 12.301$ Å, $b = 3.820$ Å, $c = 18.466$ Å, $\beta = 104.50°$) similar to that in an earlier report.[12,19] Clearly, the TTF−TCNQ nanowires in this research have the same phase but a little bit larger size than the traditionally prepared TTF−TCNQ nanowires.

Figure 2b shows the change in the UV−vis absorption of the TCNQ microstructures as a function of reaction time after mixing of the TTF microparticles and TCNQ microstructures. Clearly, the reaction between TCNQ microstructures and TTF microparticles was very fast and nearly complete within 20 s. Thus, it was not possible for us to use SEM and dynamic light scatting analysis to track the formation mechanism of TTF−TCNQ nanowires. A plausible mechanism could be given as follows: The surface of a TTF microparticle has a partial positive charge (δ^+) while the surface of a TCNQ microstructure has a partial negative charge (δ^-), as confirmed by ζ potential experiments (Figure S2). When they are mixed, the strong electrostatic attraction brings them together. A quick solid-state reaction between TTF and TCNQ could then happen, leading to the formation of TTF−TCNQ nanowires with stacking in the *b*-axis direction.

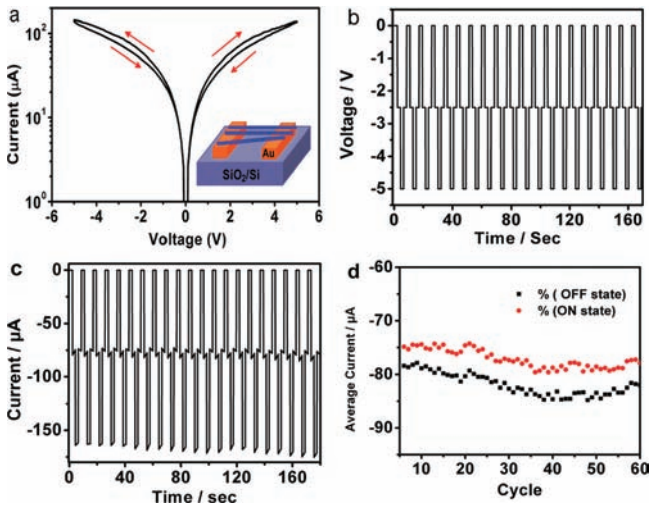

Figure 3. (a) Typical $I-V$ curves for a network of TTF−TCNQ nanowires. The inset is a schematic representation of a typical memory device. (b, c) Write−multiple-read−erase−multiple-read (WRER) cycles of a network of TTF−TCNQ nanowires for a rewritable data storage application. The writing, reading, erasing, and reading voltages were −5.0, −2.5, 0, and −2.5 V, respectively. (d) Current in the ON and OFF states as a function of the number of WRER cycles (60 cycles were tested under air conditions; the scan rate was 1.6 V/s).

The Figure 3a inset represents a typical schematic of our devices. The devices were electronically stable, and all of the current−voltage ($I-V$) measurements were performed under an air atmosphere. Figure 3a shows the typical $I-V$ characteristics of the TTF−TCNQ nanowires/Au junction. It is believed that a local nonstoichiometric composition of $TTF_{1-\delta}$−$TCNQ_1$ ($0 \le \delta \le 1$) may result in highly doped semiconducting behavior,[19c,d] although the TTF−TCNQ wire is expected to show metallic conduction along the wire axis (*b* axis). This defect might come from the different diffusion rates of TTF and TCNQ. However, such defects in the TTF−TCNQ nanowires cannot be detected by XRD because of the amount. The $I-V$ characteristics of the devices were recorded by scanning the applied voltage from 0 to +5 V and then to −5 V, followed by a reverse scan from −5 to 5 V with a scan rate of 1.6 V/s.

The obvious conductivity-switching behavior makes it possible for the devices to be used as nonvolatile rewritable organic memory devices. We believe that the switch behavior might come from the defects, which have different oxidation states. The stability of the devices was tested under a pulsed voltage sequence with a write−read−erase−read (WRER) cycle. In each cycle, the high (write) and low (erase) conducting states were repeatedly generated, and the switching states between the high- and low-conducting stages were monitored and recorded. A voltage sequence and the corresponding current from the memory device are shown in Figure 3b,c, respectively. The stable high/low (ON/OFF) conductivity-switching behavior under multiple current measurements at −2.5 V showed no significant degradation of the device with respect to either ON/OFF current or voltage after 60 write−erase cycles in air (Figure 3d). Such stable switching behavior suggests that the material has great potential for nonvolatile memory applications in which metal−semiconductor−metal junctions can be constructed.

In summary, we have successfully realized the chemical reaction between TTF microparticles and TCNQ microstructures in aqueous solution. The as-synthesized TTF−TCNQ nanowires, which are semiconducting, showed good performance in nonvolatile memory devices with multiple write−read−erase−read (WRER) cycles in air. Clearly, the postchemistry of organic particles offers a new option for preparing novel organic micro/nanostructures and tuning their physical properties. We believe that this concept can provide a more powerful tool for the design and synthesis of organic micro/nanomaterials for further applications.

Acknowledgment. The authors thank Prof. F. Wudl, Prof. M. Kanatzidis, Prof. P. Feng, and Prof. X. Bu for valuable discussions. Financial support from Nanyang Technological University (startup grant) is gratefully acknowledged.

Supporting Information Available: Details of sample preparation and device fabrication, TEM and SEM images, powder XRD characterization, ζ potential experiments, and a formation mechanism supplement for TTF−TCNQ nanowires. This material is available free of charge via the Internet at http://pubs.acs.org.

References

(1) (a) Sun, Y.; Xia, Y. *Science* **2002**, *298*, 2176. (b) Yin, Y.; Rioux, R. M.; Erdonmez, C. K.; Hughes, S.; Somorjai, G. A.; Alivisatos, A. P. *Science* **2004**, *304*, 711. (c) Vasquez, Y.; Henkes, A. E.; Bauer, J. C.; Schaak, R. E. *J. Solid State Chem.* **2008**, *181*, 1509.

(2) (a) Cui, S.; Liu, H.; Gan, L.; Li, Y.; Zhu, D. *Adv. Mater.* **2008**, *20*, 2918. (b) Zhao, Y. S.; Fu, H.; Peng, A.; Ma, Y.; Liao, Q.; Yao, J. *Acc. Chem. Res.* **2010**, *43*, 409. (c) Li, R.; Hu, W.; Liu, Y.; Zhu, D. *Acc. Chem. Res.* **2010**, *43*, 529.

(3) Fu, H.; Yao, J. *J. Am. Chem. Soc.* **2001**, *123*, 1434.

(4) (a) Liu, H.; Li, Y.; Jiang, L.; Luo, H.; Xiao, S.; Fang, H.; Li, H.; Zhu, D.; Yu, D.; Xu, J.; Xiang, B. *J. Am. Chem. Soc.* **2002**, *124*, 13370. (b) Liu, H.; Li, Y.; Xiao, S.; Gan, H.; Jiu, T.; Li, H.; Jiang, L.; Zhu, D.; Yu, D.; Xiang, B.; Chen, Y. *J. Am. Chem. Soc.* **2003**, *125*, 10794.

(5) Maynor, B. W.; Filocamo, S. F.; Grinstaff, M. W.; Liu, J. *J. Am. Chem. Soc.* **2002**, *124*, 522.
(6) Asahi, T.; Sugiyama, T.; Masuhara, H. *Acc. Chem. Res.* **2008**, *41*, 1790.
(7) Li, D.; Xia, Y. *Adv. Mater.* **2004**, *16*, 1151.
(8) Ferraris, J.; Cowan, D. O.; Walatka, V., Jr.; Perlstein, J. H. *J. Am. Chem. Soc.* **1973**, *95*, 948.
(9) (a) Ales, H.; Molinari, A. S.; Xie, H.; Morpurgo, A. F. *Nat. Mater.* **2008**, *7*, 574. (b) Kirtley, J. R.; Mannhart, J. *Nat. Mater.* **2008**, *7*, 520.
(10) Zhao, Y. S.; Wu, J.; Huang, J. *J. Am. Chem. Soc.* **2009**, *131*, 3158.
(11) Che, Y.; Datar, A.; Yang, X.; Naddo, T.; Zhao, J.; Zang, L. *J. Am. Chem. Soc.* **2007**, *129*, 6354.
(12) Liu, H.; Li, J.; Lao, C.; Huang, C.; Li, Y.; Wang, Z. L.; Zhu, D. *Nanotechnology* **2007**, *18*, 495704.
(13) Wudl, F.; Smith, G. M.; Hufnagel, E. J. *J. Chem. Soc. D* **1970**, 1453.
(14) Kim, Y. H.; Jung, S.-D.; Chung, M.-A.; Song, K. D.; Cho, D. W. *Bull. Korean Chem. Soc.* **2008**, *29*, 948.
(15) Wudl, F.; Southwick, E. W. *J. Chem. Soc., Chem. Commun.* **1974**, 254.
(16) Ziganshina, A. Y.; Ko, Y. H.; Jeon, W. S.; Kim, K. *Chem. Commun.* **2004**, 806.
(17) Long, R. E.; Sparks, R. A.; Trueblood, K. N. *Acta Crystallogr.* **1965**, *18*, 932.
(18) Batsanov, A. S. *Acta Crystallogr.* **2006**, *C62*, 501.
(19) (a) Kistenmacher, T. J.; Phillips, T. E.; Cowan, D. O. *Acta Crystallogr.* **1974**, *B30*, 763. (b) Sai, T. P.; Raychaudhuri, A. K. *Nanotechnology* **2010**, *21*, 045703. (c) Sakai, M.; Iizuka, M.; Nakamura, M.; Kudo, K. *J. Appl. Phys.* **2005**, *97*, 053509. (d) Sakai, M.; Iizuka, M.; Nakamura, M.; Kudo, K. *Jpn. J. Appl. Phys.* **2003**, *42*, 2488.

JA102154B